Progress In Electromagnetics Research, Vol. 112, 125–137, 2011

DISTINCTION OF TOOTHING AND SATURATION EFFECTS ON MAGNETIC NOISE OF INDUCTION MOTORS

J. P. Lecointe, B. Cassoret, and J. F. Brudny

Laboratoire Systèmes Electotechniques et Environnement (LSEE)
Université d'Artois, Technoparc Futura, Béthune 62400, France

Abstract—This paper focuses on the noise and vibrations of induction motors. It proposes an analytical method to distinguish the phenomenon responsible on the magnetic noise, especially the toothing and the saturation. A 3-speed 3-phase induction motor, which works sporadically at low speed for hoisting, serve as a support for experiments. Its acoustic noise during this operating mode is really important. A complete diagnosis is proposed with a 2D analytical model. The approach is progressive and it shows analytically that magnetic saturation is mainly responsible on these noise level. Then, the presented developments makes it possible to identify, in simple way, the noise components due to the both magnetic saturation and toothing effects.

1. INTRODUCTION

Analysis of vibrations and noise of magnetic origin of electrical rotating machines is difficult and requires some experience. Indeed, design methods for three phase Induction Motor (**IM**) are generally well established for conventional motors; the designers typically use analytical methods embedded in dedicated softwares While such traditional designs are nowadays routine, it should be stressed that some more difficult compromises may be needed to design a specific, less conventional, motor. This paper presents an acoustic study which is particularly challenging as it concerns an industrial three-speed three-phase **IM**. This **IM** operates mainly at two high speeds (synchronous speeds: 1500 and 3000 rpm), while the third one (375 rpm) is used only sporadically for hoisting. Designing the machine

Received 8 November 2010, Accepted 27 December 2010, Scheduled 6 January 2011
Corresponding author: Jean Philippe Lecointe (jphilippe.lecointe@univ-artois.fr).

for an intermittent mode offers certain flexibility as the rated current may be exceeded temporarily. However, at low speed, the studied motor generates a high acoustic level.

The first part of the paper describes the characteristics of the **IM** and its acoustic signature. The second part contains a study of the effects of the magnetic circuit toothing on noise. The third part determines the influence of the magnetic circuit magnetization and, in order to get a real idea of the influence of the magnetization of the stator and rotor iron on noise, results of experiments are proposed. In the last part, an original analytical method is developed to show the effects of the saturation on the emitted noise. This yields a simple analytical explanation of how the noise components appear in the acoustic spectrum, at specific frequencies. Previous studies [1, 2] have proposed models of saturated AC machines. Our approach is different from [1] because the proposed analytical model takes also into account the both toothing and saturation effects. That makes possible to identify the noise components which result either from the saturation or from the toothing or from their combination.

2. DESCRIPTION OF THE STUDIED MACHINE

The studied machine is a 50 Hz, 400 V, three phase squirrel cage **IM**. The p pole pair numbers are 1, 2 and 8 with, respectively, 19, 16 and 7.5 kW mechanical rated powers. The magnetic circuit has $N^s = 48$ stator slots and $N^r = 42$ rotor bars. The stator is equipped with a Dahlander type winding [3]. The study concerns mainly the low speed operating mode. Figure 1 shows the spectrum of the noise measured at distance of 1 meter from the stator with a microphone placed in the radial direction for rms line voltages $U^s = V^s\sqrt{3} = 395\,\mathrm{V}$. Many components with a high amplitude can be seen and the global noise exceeds 85 dBA. The components multiple of 300 Hz have the highest

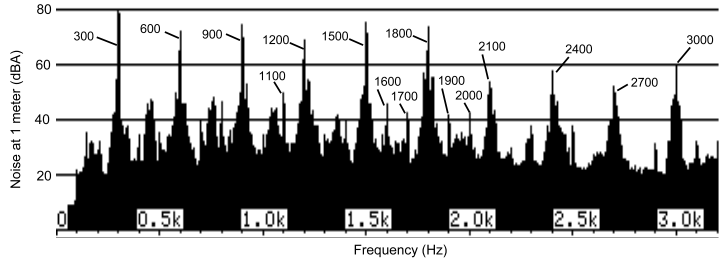

Figure 1. Acoustic spectrum for $V^s\sqrt{3} = 395\,\mathrm{V}$ and $p = 8$.

magnitude, what is rare in conventional **IM** acoustic noise. Other non negligible components multiple of 100 Hz also appear: 1100, 1600, 1700, 1900 and 2000 Hz. The stator mechanical resonance frequencies are determined in the 0–3 kHz frequency range with a modal analysis. Resonance frequencies are 290, 664, 934, 1270, 2220 Hz, ... Even if some of them are close to frequencies multiple of 300 Hz, it does not explained, contrary to other studies [2], which focuse on one excited resonance, why the noise spectrum contains such so many components of high amplitude and regularly spaced. It can be underlined that the rotation speed is very low, which precludes the hypothesis of the noise having an aerodynamic origin because such noise is proportional to the fifth power of the speed [4, 5].

3. INFLUENCE OF THE TOOTHING ON NOISE

3.1. Harmonic Analysis of the Electromagnetic Forces

The magnetic noise components result from the non static f_M per unit area Maxwell's force components [6, 7]:

$$f_M = b^2/2\mu_0 \tag{1}$$

where $\mu_0 = 4\pi 10^{-7}$ H/m is the permeability of the free space and b the radial **IM** air gap flux density:

$$b = \epsilon\lambda \tag{2}$$

ϵ and λ are respectively the airgap mmf and the per area unit airgap permeance. λ is characterized by [8]:

$$\lambda = \sum_{k_s}\sum_{k_r} \lambda_{k_s k_r} \cos\left\{ \begin{array}{l} (k_s N^s + k_r N^r)\alpha^s \\ -k_r N^r \theta - \varphi_{k_s,k_r} \end{array} \right\} \tag{3}$$

k_s and k_r are the tooth harmonic orders; they take all the values between $-\infty$ and ∞. $\lambda_{k_s k_r}$ is a coefficient, which depends on the **IM** magnetic circuit geometry. θ defines the angle between the statoric and rotoric references d^s and d^r. It depends on time t and slip s as: $\theta = (1-s)\omega t/p + \theta_0$. φ_{k_s,k_r} is tied to the position of d^s and d^r. ϵ can be expressed as:

$$\epsilon = \sum_h \hat{\epsilon}_h \cos[\omega t - hp\alpha^s - hp\varphi^s] \tag{4}$$

where:

- $h = 6k + 1$ is the space harmonic order (k being an integer, which varies from $-\infty$ to ∞)
- φ^s is a phase angle which depends on the d^s choice

- α^s is a spatial angle which allows the location of any point if the airgap relatively to d^s.

The usual assumptions, when trying to explain the magnetic noise origin of a motor supplied from the grid, is to suppose the iron relative permeability infinite and to neglect the eccentricity [4].For given three phase balanced stator voltages $v_q^s\,(q = 1, 2\,\text{or}\,3)$ of V^s rms value, one can write:

$$v_q^s = r^s i_q^s + d\psi_q^s/dt \tag{5}$$

where i_q^s is the line current which crosses the winding q, ψ_q^s the flux linked to it and r^s the resistance winding.

The determination of b is done at no load. In this condition, the rotor currents can be assumed to be null and the stator currents are identified with the magnetizing currents. Moreover, if $r^s i_q^s$ is neglected and as ψ_q^s comes from b, using integration, it appears that b is directly linked to v^s. Sinusoidal i_q^s currents of ω angular frequency are considered. Neglecting the phase angles, b can be written as:

$$b = \sum_h \sum_{k_s} \sum_{k_r} \hat{b}_{h,k_s,k_r} \cos(\omega_b t - M_b \alpha^s) \tag{6}$$

where f_M, given by (1), can be expressed as:

$$f_M = \sum_W \sum_m f_{W,m} = \sum_W \sum_m \hat{f}_{W,m} \cos(Wt - m\alpha^s) \tag{7}$$

So, the force components rotate at the speed W/m where W is the angular frequency of the force component ($W = 2\pi F$) and the m mode number indicates the number of attraction points between the stator and the rotor [9]. Low values of m are the most unfavorable because, for $m \geq 2$, the stator vibration amplitudes generated by the forces are linked to $1/m^4$ [5]. The product of two flux density components includes:

- the term square defined by f_{W_0,m_0} with $W_0 = 2\omega_b$ and $m_0 = 2M_b$
- the double products for which two flux harmonics are differentiated by indexes 1 and 2. Such components are defined by f_{W_1,m_1} and f_{W_2,m_2} with $W_1 = \omega_{b_1} + \omega_{b_2}$, $m_1 = M_{b_1} + M_{b_2}$, $W_2 = \omega_{b_1} - \omega_{b_2}$ and $m_2 = M_{b_1} - M_{b_2}$.

These forces deform the mechanical structure of the stator, especially its external housing. These deformations generate pressure variations of the air, leading to acoustic noise waves. A force amplitude is function of $\hat{f}_{W,m}$ and m but also of the mechanical response of the stator structure, especially if F is close to a resonance frequency [10–12]. Therefore, empirical law have been developed to model the link

between the forces, the vibrations and the acoustic noise [5]. The mechanical models assimilate generally the stator as a ring so that the static and dynamic displacements can be calculated. Analytical acoustic models consider the machine as a sphere or a cylinder of infinite length to calculate the acoustic pressure from the stator displacements.

3.2. Influence of Tooth and Space Harmonics

As $N^s = 6p$ and $N^r = 5.25p$ and considering the studied machine with $p = 8$, it can be written:

$$W_0 = [1 - 5.25k_r(1 - s)]2\omega \tag{8}$$

$$m_0 = 2p(1 + 6K - 5.25k_r) \tag{9}$$

$$W_1 = [2 - 5.25k_{(r+)}(1 - s)]\omega \tag{10}$$

$$m_1 = p(2 + 6K_{(+)} - 5.25k_{(r+)}) \tag{11}$$

$$W_2 = [-5.25k_{(r-)}(1 - s)]\omega \tag{12}$$

$$m_2 = p(6K_{(-)} - 5.25k_{(r-)}) \tag{13}$$

where:

- $k_{(r+)} = k_{r1} + k_{r2}$,
- $k_{(r-)} = k_{r1} - k_{r2}$,
- $k_{(s+)} = k_{s1} + k_{s2}$,
- $k_{(s-)} = k_{s1} - k_{s2}$,
- $h_1 + h_2 = 2 + 6h_{(+)}$,
- $h_1 - h_2 = -6h_{(-)}$,
- $K = h - k$,
- $K_{(+)} = h_{(+)} - k_{(s+)}$,
- $K_- = h_{(-)} + k_{(s-)}$,
- h, k_s and k_r vary between $-\infty$ and $+\infty$.

Considerations about m and F allow one to determine the dominant force components. m is an integer, which value is limited to 8 according to the previous comments about the noise vibrations. The results shown at Table 1 present frequencies up to 3 kHz with $s = 0$. However, one can see that these components are not preponderant in the spectrum of Fig. 1 except the line of 2100 Hz frequency. This first analytical model does not explain why force components of frequency multiple of 100 and 300 Hz are responsible for noise.

In order to check the validity of the analytical determination, measurements have been done for $p = 2$ in the same conditions as

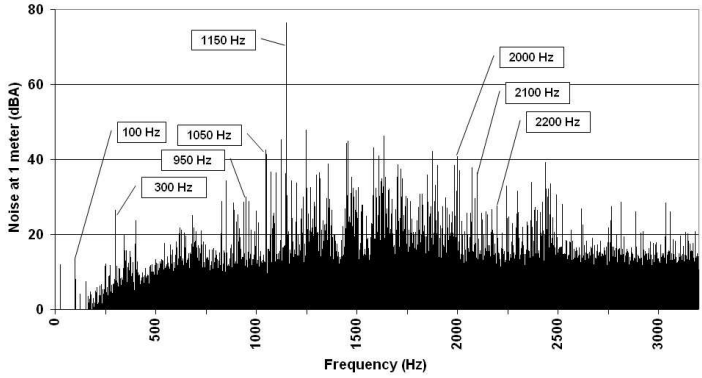

Figure 2. Acoustic spectrum for $V^s\sqrt{3} = 395\,\mathrm{V}$ and $p = 2$.

Table 1. Toothing force components ($p = 8$).

F_0	m_0	F_1	m_1	F_2	m_2
625	4	625	4	262.5	6
1150	8	887.5	8	1837.5	6
		950	8	2100	0
		1150	8	2362.5	6
		1212.5	2		
		1475	4		
		2725	4		
		2987.5	2		

Table 2. Force components created by the toothing $p = 2$.

F_0	m_0	F_1	m_1	F_2	m_2
100	4	100	4 and 8	1050	6
1150	2	950	2	2100	0
2000	8	1150	2		
2200	8	2000	4 and 8		
		2200	4 and 8		

for the low speed (Fig. 2) and the analytical model has been applied (Table 2). It is important to notice that all the components determined analytically can be found in the noise spectrum, except the 2200 Hz component which presents a high m value. It can be seen that the 1150 Hz ($m = 2$) component presents the highest amplitude. On the one hand, it confirms the validity of the model to determine the noise due to the toothing and, on the other hand, it reveals the necessity to extend it in order to explain the noise measured with $p = 8$.

4. INFLUENCE OF THE SATURATION

The noise can be explained by an abnormal saturation of the magnetic circuits. Following parts present a verification of the stator design and

the variation of the noise with different values of V^s.

4.1. Validity of the Stator Design at Low Speed

The first approach consists in validating the electromagnetic design for the low speed and sinusoidal variations of the airgap flux density. So, only the term corresponding to $h = 1$ and $k_s = k_r = 0$ in Equation (6) is considered ($b = b_1$). The average flux ϕ under a pole is given by (14) where D and L are the internal diameter and the length of the stator magnetic circuit respectively ($D = 0.165\,\text{m}$ and $L = 0.225\,\text{m}$).

$$\bar{\phi} = DL\hat{b_1}/p \tag{14}$$

When the traditional design of three phase machines is used, neglecting the saturation, one can obtain:

$$V^s = 2.22\pi K_1 n^s f\bar{\phi}/\sqrt{2} \tag{15}$$

where:

- K_1 is the winding factor. As the number of slots per phase and per pole is equal to 1 for $p = 8$, $K_1 = 1$
- n^s is the number of wires in the slot per phase series connected: $n^s = 216$
- $V^s = 230\,\text{V}$

The calculation leads to $\bar{\phi} = 9.59\,\text{mWb}$ and $\hat{b_1} = 2.07\,\text{T}$, a value which is obviously theoretical insofar saturation is not taken into account. Although it depends on the quality of the sheets, the magnetic circuit will be saturated below the calculated value. A designer usually chooses $\hat{b_1} = 0.7\,\text{T}$.

Then, considering $\hat{b_1} = 2.07\,\text{T}$ leads to define the flux density in the stator teeth: 6 T. In reality, for turbogenerators with grain oriented laminations [13], the maximum value of the flux density in the teeth is 2.1 T. As a consequence, theses two calculations show that the machine is very saturated. Moreover, the magnetizing current is close to the rated current; that confirms the saturation. The next step consists in checking the saturation effect and its impact on the acoustic noise.

4.2. Experimental Validation

In order to confirm that the saturation level and so the magnetic noise depend on V^s, a simple experiment has been conducted by decreasing V^s and measuring the noise at no load. Such measurements have been done for $V^s\sqrt{3} = 370\,\text{V}$ and 350 V. The rotor speed is not significantly modified by the voltage decreasing. The acoustic spectra measured at

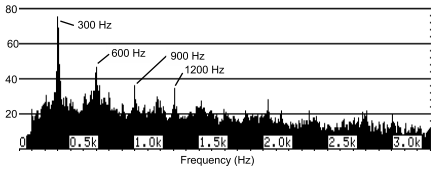

Figure 3. Acoustic spectrum for $V^s\sqrt{3} = 370\,\mathrm{V}$ and $p = 8$.

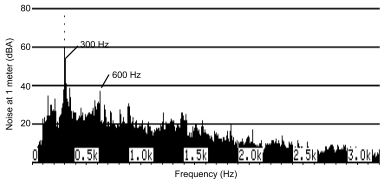

Figure 4. Acoustic spectrum for $V^s\sqrt{3} = 350\,\mathrm{V}$ and $p = 8$.

Table 3. Variation of the acoustic line amplitude versus V^s.

$V^s\sqrt{3}$	F (Hz)				
	300	600	900	1200	1500
395	84	71.9	74.3	69.1	75.3
370	75.4	46.6	35.9	32.2	21.6
	(−10%)	(−35%)	(−51%)	(−53%)	(−71%)
350	59.4	31	29.1	25.7	19.7
	(−29%)	(−56%)	(−60%)	(−62%)	(−73%)

1 m away from the machine are shown in Figs. 3 and 4. The noise decrease is drastic and the global noise follows the level of the 300 Hz line. The amplitude of that line is 84 dBA with a voltage supply of $V^s\sqrt{3} = 395\,\mathrm{V}$; it is equal to 75 dBA with 370 V and it is under 60 dBA with 350 V. The next 5 lines (600, 900, 1200, 1500 and 1800 Hz) present the same variations: their amplitudes are above 69.1 dBA with 395 V and they do not exceed 46.6 dBA and 30.3 dBA respectively with 370 and 350 V. The Table 3 shows the decreasing of the major lines. Are shown in percent the decreasing of the noise line amplitudes (dBA) relatively to the level obtained with 395 V. The decreasing of the forces, for a non saturated machine, should decrease with $(V^s)^2$. So, the force component amplitudes should be linearly decreased by 12% and 21% when $V^s\sqrt{3} = 370\,\mathrm{V}$ and 350 V. The variation of the noise components (in dBA) are higher, which means force component amplitudes are drastically reduced. For the 300 Hz component, force amplitude is decreased by 62% and 94% for $V^s\sqrt{3} = 370\,\mathrm{V}$ and 350 V. At last, the components of frequency multiple of 100 Hz and different from 300 Hz disappear completely when $V^s\sqrt{3} = 350\,\mathrm{V}$.

5. ANALYTICAL MODELING OF SATURATION

5.1. Modelling Method

Let us consider first a smooth airgap machine, which iron permeability is infinite. Let us denote g the airgap thickness and ϵ_1 the mmf fundamental component. According to Equation (2), such assumptions lead to a sinusoidal airgap flux density b_1 as shown in Fig. 5. The magnetic field lines, which cross the airgap, go through the statoric and rotoric iron. b_{iron} denotes the corresponding iron flux density. If parts of the iron are saturated ($b_{iron} > B_{iron}^{sat}$), it means that no negligible ampere-turns are consumed by iron (teeth and yokes), decreasing the airgap mmf [1]. As b_{iron} is linked to b_1, one can associate to B_{iron}^{sat} the quantity E^{sat}, which corresponds to the value of ϵ_1 over which some parts of the iron become saturated. One can assume that ϵ_1 becomes ϵ^{sat} as shown in Fig. 6(a). The airgap flux density b^{sat} results from the product $\epsilon^{sat}\lambda_{00}$. However, to make the calculation easier, this phenomenon can be modeled by keeping the airgap fmm equal to ϵ_1 and by modifying the airgap thickness so that the airgap permeance

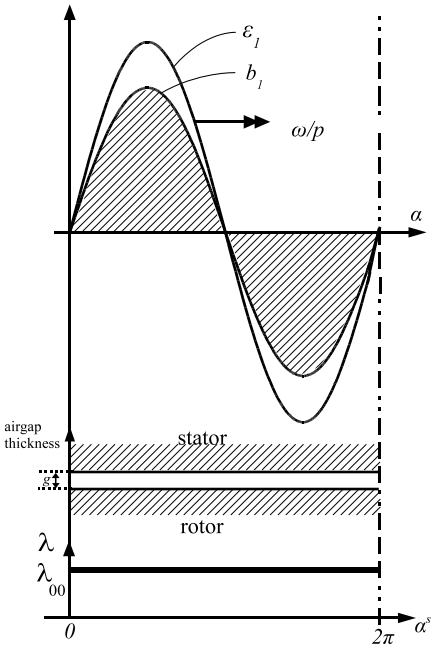

Figure 5. Model without saturation.

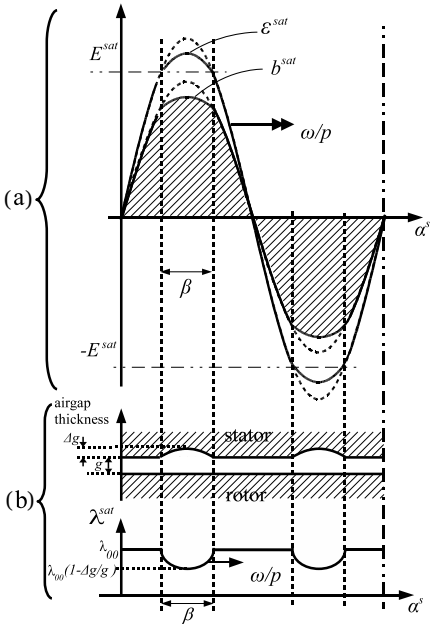

Figure 6. Model with saturation.

becomes λ^{sat} as shown in Fig. 6(b). Assuming that the fictitious airgap thickness varies between g and $g + \Delta g$, λ^{sat} varies between μ_0/g and $\mu_0/(g + \Delta g)$. For $\Delta g = g$, the theoretical 2.07 T value previously calculated becomes 1.03 T. So, there is an important decreasing of the saturation effect and, consequently, one can admit that $\Delta g < g$. In these conditions, it can be assumed that λ^{sat} varies between λ_{00} and $\lambda_{00}(1-\Delta g/g)$. Let us introduce the angle β, which takes no null values when $\hat{\epsilon_1} > E^{sat}$. The value of Δg increases when $\hat{\epsilon_1} - E^{sat}$ increases.

5.2. Force Components

For a given value of V^s, it can be assumed that β, which characterizes the saturated iron parts, and Δg, which characterizes the decreasing of λ (Fig. 6(b)), are constant. In order to express the permeance by unit area of a saturated machine, one can first neglect the toothing so that the λ^{sat} wave given in Fig. 6(b) can be expressed as (16) where $\lambda_{00}^{sat} < \lambda_{00}$.

$$\lambda^{sat} = \lambda_{00}^{sat} - \sum_{h'=1}^{\infty} \delta_{h'} cos(2h'\omega t - 2ph'\alpha^s) \tag{16}$$

Then, the toothing is taken into account by replacing, with an adaptation of the coefficients, λ_{00}^{sat} with the relationship (3):

$$\lambda^{sat} = \left\{ \begin{array}{l} \displaystyle\sum_{k_s} \sum_{k_r} \lambda_{k_s k_r}^{sat} \cos \left\{ \begin{array}{l} (k_s N_s + k_r N_r)\alpha^s \\ -k_r N_r \theta \end{array} \right\} \\ \displaystyle - \sum_{h'=1}^{\infty} \delta_{h'} cos(2h'\omega t - 2ph'\alpha^s) \end{array} \right\} \tag{17}$$

$\delta_{h'}$ models the harmonic amplitude of saturated parts. Calculation of the flux density leads to expression similar to (6). The terms resulting from the double sum are marked with $*$ and they are defined by:

- $\omega_{b^*} = [1 - 5.25(1 - s)k_r]\omega$
- $M_{b^*} = 8[1 + 6(k_s - k_r) - 5.25k_r]$.

The terms resulting from the product of the second group of expression (17) with ϵ are marked with $**$ and they are characterized by:

- $\omega_{b^{**}} = [1 + 2h']\,\omega$
- $M_{b^{**}} = 8\,[h + 2h']$.

Calculations of the force components lead to the quantities W_0, m_0, W_1, m_1, W_2, m_2 if the square of b^* and the double products

between the terms of b^* are considered. Moreover, additional components appear because of b^{**}. Their characteristics are shown at Table 4 where:

- $k_{(+)} = k_1 + k_2$,
- $k_{(-)} = k_1 - k_2$,
- $h'_{(+)} = h'_1 + h'_2$ and
- $h'_{(-)} = h'_1 - h'_2$.
- the components resulting from square of b^{**} are identified with W_0^{sat}, m_0^{sat},
- the components obtained from the double products between the terms of b^{**} are characterized by:
  - $\left\{W_1^{sat}, m_1^{sat}\right\}$ and
  - $\left\{W_2^{sat}, m_2^{sat}\right\}$
- the components which result from the double product between terms of b^* and b^{**} are identified with $\left\{W_3^{sat}, m_3^{sat}\right\}$ and $\left\{W_4^{sat}, m_4^{sat}\right\}$.

Let us analyse these new components when $p = 8$.

- Concerning m_0^{sat}, as h is odd and $2h'$ is even, the lowest mode number is 16. Thus, components defined with W_0^{sat} and m_0^{sat} have no significant effect.
- Contrary to m_0^{sat}, m_1^{sat} can be null, which leads to $h'(+) = -1 - 3k_{(+)}$ and $W_1^{sat} = -6k_{(+)}\omega$. Therefore, this component, which results from the combination of harmonics linked to b^{**},

Table 4. Force components due to the saturation.

$W_0^{sat} = (1 + 2h')2\omega$	
$m_0^{sat} = 16(h + 2h')$	
$W_1^{sat} = [1 + h'_{(+)})]2\omega$	multiple of 300Hz
$m_1^{sat} = 16[1 + 3k_{(+)} + h'_{(+)}]$	multiple of 300Hz
$W_2^{sat} = 2h'_{(-)}\omega$	multiple of 300Hz
$m_2^{sat} = 16[3k_{(-)} + h'_{(-)}]$	multiple of 300Hz
$W_3^{sat} = [2 - 5.25(1 - s)k_r + 2h']\omega$	multiple of 100Hz
$m_3^{sat} = 8[2 + 6(k_{(+)} - k_s) + 2h' - 5.25k_r]$	multiple of 100Hz
$W_4^{sat} = [-5.25(1 - s)k_r - 2h']\omega$	multiple of 100Hz
$m_4^{sat} = 8[6(k_{(-)} - k_s) + 2h' - 5.25k_r]$	multiple of 100Hz

has a frequency multiple of 300 Hz and a mode number equal to 0. The same conclusion can be drawn for W_2^{sat} and m_2^{sat}.

- m_3^{sat} and m_4^{sat} correspond, if $h' = 0$, to components characterized by m_1 and m_2. As $h' \neq 0$, they contribute to add, at no load, noise components of frequency multiple of 100 Hz (for example 1100, 1600, 1700, 1900 and 2000 Hz on the spectrum of Fig. 1).

6. CONCLUSION

An industrial three phase three speed induction motor, which is very noisy when it operates at low speed, has been studied. An analytical model considering hypotheses of non saturation shows that the toothing is not alone responsible on this important noise of magnetic origin. Then, a simple design approach and experiments have shown that the magnetic circuit is very saturated. An extended analytical model of forces when magnetic circuit is saturated is proposed. It allows explaining clearly what kinds of force components are responsible for the major noise components. Moreover, toothing and saturation effects can be decoupled with simple analytical expressions. The proposed analytical developments constitutes a tool easily usable to explain the noise of **IM**.

REFERENCES

1. Moreira, J. C. and T. A. Lipo, "Modeling of saturated ac machines including air gap flux harmonic component," *IEEE Trans. on Ind. Appl.*, Vol. 28, No. 2, 343–349, 1992.
2. Le Besnerais, J., V. Lanfranchi, M. Hecquet, G. Lemaire, E. Augis, and P. Brochet, "Characterization and reduction of magnetic noise due to saturation in induction machines," *IEEE Trans. on Mag.*, Vol. 45, No. 4, 2003–2008, 2009.
3. Mauduit, A., *Machines Electriques*, Tome II, Paris, 1931.
4. Cassoret, B., R. Corton, R. Roger, and J. F. Brudny, "Magnetic noise reduction of induction motors," *IEEE Trans. on Power Electronics*, Vol. 18, No. 2, 570–579, 2003.
5. Jordan, H., *Geruscharme Elektromotoren*, W. Girardet, Essen, 1950.
6. Mininger, E., E. Lefeuvre, M. Gabsi, C. Richard, and D. Guyomar, "Semiactive and active piezoelectric vibration controls for switched reluctance machine," *IEEE Trans. on Energy Conversion*, Vol. 23, No. 1, 78–85, 2008.

7. Alger, P. L., "The magnetic noise of polyphase induction motors," *IEEE Trans. Amer.*, Vol. 73, No. 3, 118–125, 1954.
8. Brudny, J. F., "Modelling of induction machine slotting resonance phenomenon," *European Physical Journal, Applied Physic., JPIII*, 1009–1023, 1997.
9. Hubert, A. and G. Friedrich, "Influence of the power converter on induction motor acoustic noise interaction between the control strategy and the mechanical structure," *IEE Proc. — Electr. Appl.*, Vol. 149, No. 2, 93–100, 2002.
10. Ostovic, V. and G. Boman "Radial air gap force as a source of audible noise in a sinusoidally fed induction motor," *Conference Record of the 1995 IEEE Industry Applications Conference*, Vol. 1, 591–598, 1995.
11. Huang, K. S., Z. G. Liu, Li, H., J. Yang, D. R. Turner, L. Jiang, and Q. H. Wu, "Reduction of electromagnetic noise in three-phase induction motors," *International Conference on Power System Technology Proceedings (PowerCon)*, Vol. 2, 745–749, 2002.
12. Lecointe, J. P., R. Romary, J. F. Brudny, and T. Czapla, "Five methods of stator natural frequency determination," *Mechanical Systems and Signals Processing*, No. 18, 1133–1159, 2004.
13. Lecointe, J. P., S. Duchesne, J. F. Brudny, and J. Y. Roger, "Retro-design of turbogenerators. Part 2: determination of the stator geometry," *Electric Machines and Drives Conference*, Vol. 2, 1008–1013, 2007.